Two-neutron transfer in Pt nuclei and the structure of ^{200}Pt

J. A. Cizewski,* E. R. Flynn, Ronald E. Brown, D. L. Hanson,† S. D. Orbesen, and J. W. Sunier
Los Alamos Scientific Laboratory, Los Alamos, New Mexico 87545
(Received 10 October 1980)

The ^{194,196,198}Pt(t,p) reactions have been measured with 17 MeV tritons on enriched and natural Pt targets. The level structure of ^{200}Pt is probed for the first time, and several new excited 0^+ states have been identified in ^{196,198,200}Pt. Systematics in level structure of $^{192-200}$Pt are fairly constant, although there is evidence that ^{198,200}Pt are becoming more vibrational in structure, with the γ-unstable shape of the lighter Pt nuclides becoming more oblate-like. Systematics of $L = 4$ strengths are considered and can be qualitatively understood. The (t,p) strengths measured in the present study are combined with earlier Pt(p,t) and Os(t,p) measurements and compared with the systematics of two-neutron transfer strengths predicted by the interacting boson approximation, schematic, boson expansion, and pairing vibration models.

[NUCLEAR REACTIONS ^{194,196,198}Pt(t,p), $E=17$ MeV; enriched targets; measured energy levels, $\sigma(\theta)$ in ^{196,198,200}Pt; DWBA.
NUCLEAR STRUCTURE $L=4$ transitions, interacting boson approximation model, schematic model, boson expansion technique, pairing vibration model.]

I. INTRODUCTION

For many years there has been interest in performing two-neutron transfer studies in nuclei near closed shells in order to investigate pairing vibrational excitations. The recent development of the interacting boson approximation (IBA) (Refs. 1–3) model by Arima and Iachello has extended the ability to understand particle pair correlations by a boson description of mid-shell and transitional nuclei with $A \gtrsim 100$. Included in this model is the ability to relate empirical and predicted strengths of collective $L = 0$ and $L = 2$ transitions in spherical, deformed, and transitional nuclei. In the Pt nuclei it has been shown[4] that ^{196}Pt is an excellent empirical example of the O(6) (Ref. 3) limiting symmetry of the IBA. The key signature of this symmetry is sequences of 0^+-2^+-2^+ levels connected by $E2$ transitions. The (t,p) reaction is ideal for identifying 0^+ states, and such states are often difficult to recognize unambiguously in most other nuclear reactions.

Another aspect of nuclear structure probed in (t,p) studies is the level schemes of neutron-rich nuclei, which are difficult to populate in other reactions. In the present study we have been able to extend the knowledge of ^{198}Pt and provide the first investigation of excited states in ^{200}Pt. Since the Pt nuclei lie in a transitional region between the well-deformed rare earth nuclei and the closed shell Pb nuclei, an understanding of the Pt nuclei involves a better understanding of how this shape change progresses. Studying ^{200}Pt, which is only four neutrons away from the $N = 126$ closed shell, fills in a gap in the systematics of this transitional region.

In Sec. II we will present our experimental technique, followed in Sec. III by the level energies and spin assignments which can be deduced from the present study in combination with earlier measurements. In the discussion of Sec. IV, the level systematics, two-neutron transfer strengths, and the implications of these for the IBA and other models will be presented. Some of these topics have been discussed in an earlier publication.[5]

II. EXPERIMENTAL PROCEDURES

The (t,p) reactions on enriched and natural Pt targets were performed with a 17-MeV triton beam from the Los Alamos Scientific Laboratory Tandem Van de Graaff accelerator. The reaction protons were momentum analyzed using the LASL Q3D (quadrupole-dipole-dipole-dipole) spectrometer[6] and detected with a helical proportional chamber[7] in the focal plane of the Q3D. Typical spectra are shown in Figs. 1–3.

The enriched targets of ^{194}Pt(97.41%), ^{196}Pt(97.28%), and ^{198}Pt(95.83%) were self-supported sputtered foils of 150–250 μg/cm^2 in thickness. The natural Pt and Os targets were also self-supported sputtered targets of 150–200 μg/cm^2 in thickness. For the enriched targets, angular distribution measurements were taken between 10° and 60° in 5° steps with the full solid angle (14.3 msr) of the Q3D spectrometer. A surface barrier detector placed at approximately 30° detected the elastically scattered tritons in order to normalize the measurements at each angle. We were able to obtain absolute cross sections after determining the target thickness from optical model predictions. In order to obtain the most ac-

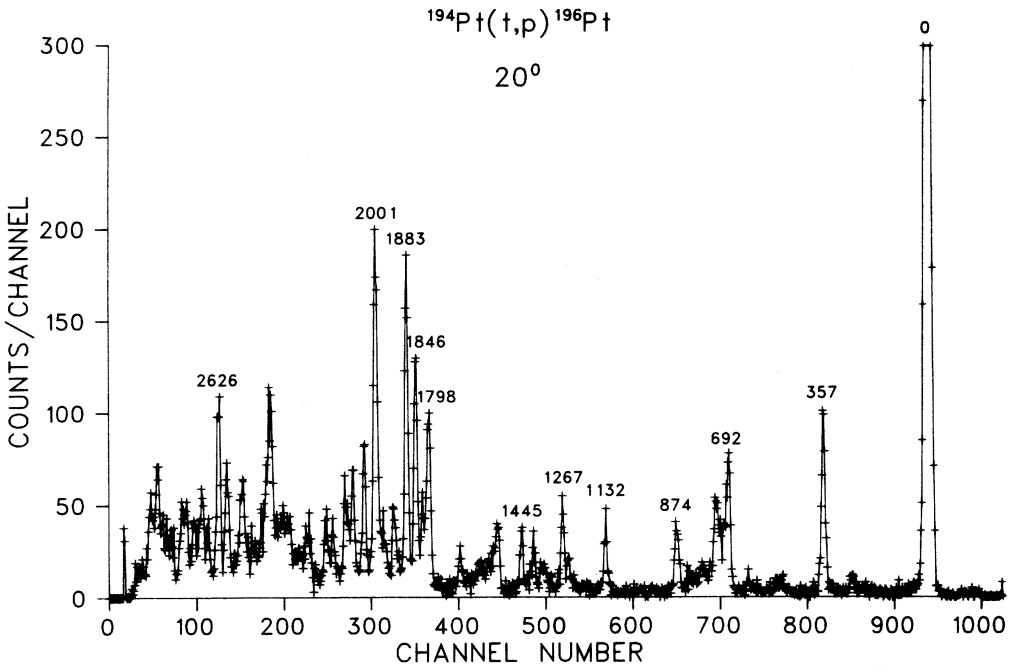

FIG. 1. Spectrum of the ^{194}Pt$(t,p)^{196}$Pt reaction measured at 20° with 17 MeV tritons. Several states are labeled by the excitation energies in keV as determined in the present study.

curate relative ground-state cross sections, measurements were also performed on natural Pt and Os targets at 25°, 30°, and 50°, the positions of maxima in $L = 0$ angular distributions.

The means of obtaining the energy calibration was different for each target. For the ^{194}Pt(t,p) reaction, the well-established excitation energies in ^{196}Pt from a recent (n,γ) measure-

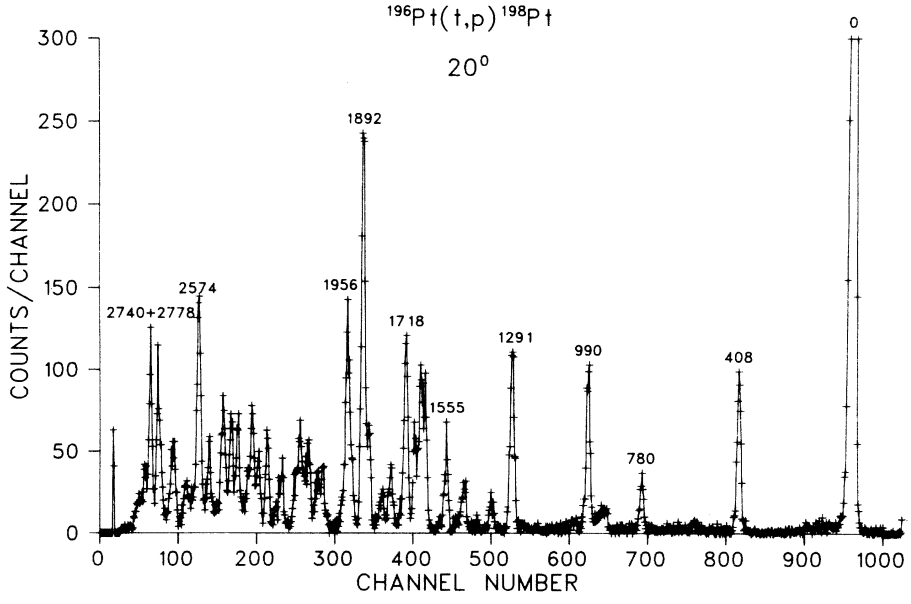

FIG. 2. Spectrum of the ^{196}Pt$(t,p)^{198}$Pt reaction. See caption to Fig. 1.

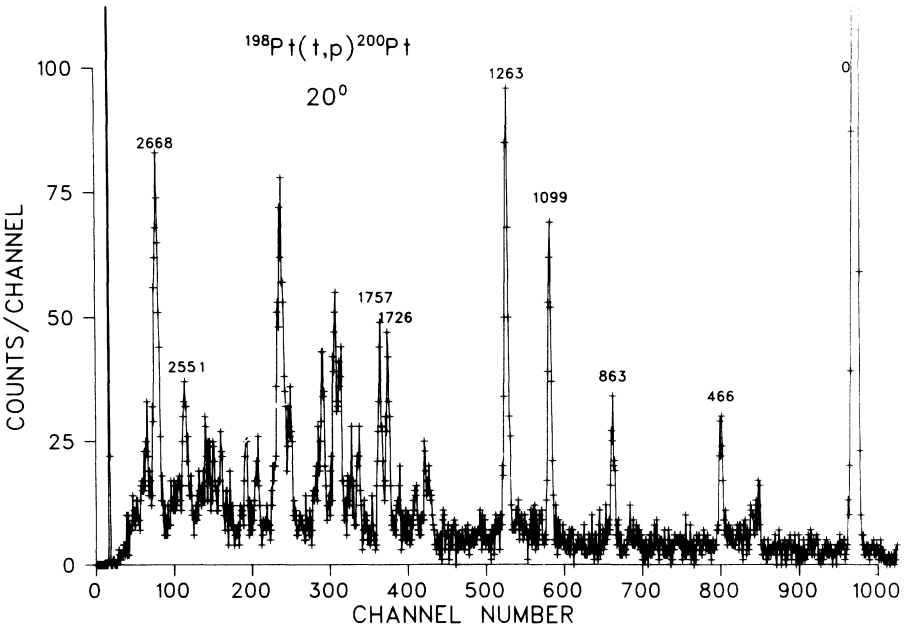

FIG. 3. Spectrum of the ^{198}Pt$(t,p)^{200}$Pt reaction. See caption to Fig. 1.

ment[8] were used to internally calibrate the (t,p) measurement. Above ~2 MeV in excitation the level density is so high that the correlation between states populated in (n,γ) and (t,p) is not unambiguous, as reflected in our stated errors. The ^{196}Pt$(t,p)^{198}$Pt reaction energy calibration was obtained by measuring the ^{192}Os$(t,p)^{194}$Os reaction[9] under identical magnetic field and angle configurations. The ^{196}Pt$(t,p)^{198}$Pt ground-state Q value agrees with the earlier value of 4.930 MeV. Due to the larger errors on the ^{194}Os excitation energies, the ^{198}Pt energies quoted also have sizable errors, but agree with the excitation energies measured in Coulomb excitation[10] and concurrent ^{198}Pt$(n,n'\gamma)$ (Ref. 11) and ^{198}Pt(p,p') (Ref. 12) investigations. The ^{198}Pt$(t,p)^{200}$Pt reaction was calibrated with the ^{194}Pt$(t,p)^{196}$Pt reaction, using the energies from the (n,γ) study.[8] The ^{198}Pt$(t,p)^{200}$Pt ground-state Q value obtained was 4.356 ± 0.020 MeV, giving a mass excess for ^{200}Pt of −26.616 ± 0.020 MeV, in agreement with the prediction from systematics of Wapstra and Bos[13] of −26.600 MeV.

The levels populated in the (t,p) reaction on ^{194}Pt, ^{196}Pt, and ^{198}Pt are summarized in Tables I–III, respectively. Included are the excitation energies and differential cross sections at 25° measured in the present study. For the ^{196}Pt and ^{198}Pt final nuclei, we have also summarized the information from earlier investigations and, in the case of ^{196}Pt, have given the more restrictive J^{π} values which can now be assigned. The experimental angular distributions for the ^{194}Pt, ^{196}Pt, and ^{198}Pt targets are presented in Figs. 4–6.

The ground-state transitions in Pt and Os (t,p) were also measured with natural targets in order to obtain relative transition strengths of higher accuracy. Although these natural target measurements have been reported previously,[5] for completeness and for the later discussion the information from the natural targets is summarized in Table IV.

III. DISTORTED-WAVE BORN APPROXIMATION (DWBA) CALCULATIONS

The experimental angular distributions presented in Figs. 1–3 for the Pt (t,p) measurements were compared with the predictions of the DWBA code[15] DWUCK 4. The triton optical model parameters[16] used were those of Flynn and co-workers. The proton parameters[17] were essentially those of Perey, except that the real well depth of the proton potential had to be slightly modified (~4 MeV) to better reproduce the empirical positions of the minima in the $L=0$ ground state transitions. The parameters are summarized in Table V.

The identification of $L=0$ transitions in (t,p) reactions is straightforward due to the pronounced minima in the angular distributions, at ~15° and ~40° in Pt(t,p). However, for other angular momentum transfers the assignments are more difficult. DWBA calculated angular distributions for

TABLE I. States populated in ^{194}Pt(t,p) ^{196}Pt.

E_x (keV)[a] (t,p)	$d\sigma/d\Omega$ (μb/sr)[b] (25°)	L[c]	E_x (keV)[d] (n,γ)	J^π (n,γ)	J^π[e] adopt
0	362(11)	0	0.000	0^+	0^+
357(3)	7.9(7)		355.684	2^+	2^+
692(3)	5.5(6)	(2)	688.672	2^+	2^+
874(3)	8.5(7)	(4)	867.852	4^+	4^+
1132(3)	7.4(7)	0	1135.292	0^+	0^+
1267(3)	2.9(5)		1270.198	$5^-(3^-)$	$5^-(3^-)$
1291(3)	6.6(7)	(4)	1293.291	4^+	4^+
1363(3)	2.1(4)		1361.566	2^+	2^+
1401(3)	6.1(6)	0	1402.704	0^+	0^+
1445(3)	5.0(6)		1447.027	3^-	3^-
1537(4)	3.9(5)		1537[f]		
1601(6)	1.0(6)		1604.471	2^+	2^+
1676(3)	3.6(10)		1677.222	2^+	2^+
1798(3)	13.1(15)		1795.08	$2^+(1^-)$	$2^+(1^-)$
1819(5)	12.5(15)	0	1823.21	0^+	0^+
1846(3)	8.5(13)	(2)	1847.326	2^+	2^+
1883(3)	24(2)	(4)	1884[g]	(4^+)	(4^+)
1916(8)[h]	4.9(8)		1918.497	$0^+(1^+)$	0^+
1935(5)[h]	3.1(8)		1932.00	$0^+,2^+(1^+)$	$0^+,2^+(1^+)$
(1971(8)[i]	1.1(6))				
2001(3)[j]	26(2)	(4)			(4^+)
2047(3)	9.0(14)	(2)	2046.96	$1^+(2^+)$	2^+
2092(3)	6.8(10)	(2)	2093.0	$0^+,1^+,2^+$	2^+
2120(3)	5.9(9)				
2169(3)	4.2(7)				
2196(3)	7.5(8)	0	2199.417	$0^+,2^+(1^+)$	0^+
2267(6)	3.1(6)	(2)	2262.401	2^+	2^+
			2270.2	$0^+,1^+,2^+$	$0^+,1^+,2^+$
2305(8)	2.1(5)	(2)	2309.190	$1^+,2^+$	$2^+(1^+)$
2326(8)	2.1(5)		2324.205	$1^+,2^+$	$2^+(1^+)$
2419(5)	2.3(15)		2422.490	$0^+,2^+$	$0^+,2^+$
2449(7)	4.1(20)		2443.9	2^+	2^+
2489(8)	1.3(13)		2488.211	$1^+,2^+$	$2^+(1^+)$
2529(5)	9(3)				
2591(5)	6.0(11)	(2)	2586.9	$0^+,1^+,2^+$	$0^+,1^+,2^+$
			2599.1	$0^+,2^+(0^-,1^-,2^-)$	$0^+,2^+(0^-,1^-,2^-)$
2626(5)	10.9(15)	(2)	2629.9	$0^+,2^+(0^-,1^-,2^-)$	$2^+(1^-)$
2667(5)	4.1(7)		2667.132	2^+	2^+
2694(5)	5.2(8)				
2723(5)	2.8(7)				
2756(5)	3.9(10)				
2774(5)	6.5(11)				
2817(6)	3.6(7)				
2834(5)	3.4(7)				
2873(5)	5.1(8)	(2)			

[a] Excitation energy in keV as measured in the present (t,p) study. Errors in parentheses are on the last digit(s).

[b] Cross section at 25° in μb/sr. Errors in parentheses reflect only relative errors on the last digit(s). There is an additional 15% error in determining absolute cross sections.

[c] Transferred L value determined in the (t,p) investigation.

[d] Excitation energy in keV and J^π values as measured in the earlier (n,γ) study of Ref. 8, except as noted.

[e] J^π values which may be adopted based on the earlier (n,γ) measurements and the present (t,p) results. It was assumed that states populated with >3 μb/sr cross section at 25° are natural parity states.

[f] The 1537 keV level was also observed in the (p,t) measurement of Ref. 13. The character of this state is unknown. It is probably not the 1525 keV 6^+ state seen in the Coulomb excitation of Ref. 10 because of the large energy discrepancy.

TABLE I. (*Continued*)

[g] The 1884 keV level was seen in (p,t) and assigned (4^+) in Ref. 14.

[h] The 1916+1935 keV doublet could not be unambiguously separated at all angles. The angular distribution of the summed peak is presented in Fig. 4. The intensity of the 1916 keV transition and the portions of the angular distribution which could be extracted are consistent with the 0^+ J^π value adopted. The 1935 keV component of this doublet is too weak to permit further spin restrictions than given in (n,γ).

[i] The 1971 keV level is tentatively assigned to ^{196}Pt, since it could not be extracted at back angles and is quite weak at forward angles. The angular distribution for this state is not presented in Fig. 4.

[j] Above ~2 MeV the correspondence between levels seen in (t,p) and (n,γ) is not unambiguous due to the high level density. Therefore, except for the 2199 keV level, the (t,p) and (n,γ) correspondences should be considered tentative.

$L=0$ and $L=2$ transfers are shown in Figs. 4–6. The calculations were averaged over the ±3.0° acceptance angle of the Q3D. As is frequently the case in heavier nuclei, the predicted $L=2$ shape and that observed for the first $2^+(2_1^+)$ state are radically different, presumably due to two-step processes involving the inelastic excitation of the 2_1^+ state. However, for the 2_2^+ state the DWBA fit to the data is reasonable, and therefore, tentative $L=2$ transfer assignments can be made in several cases. For higher L values, such as $L=4$, the predicted angular distributions are essentially structureless, as opposed to the data for known[8,14] 4^+ states in ^{196,198}Pt. Therefore, we have used the empirical shape of the known[8] 1291-keV 4^+ transition in ^{196}Pt to aid in the identification of 4^+ states, as indicated by the dashed curves in Figs. 4–6. The L values we have assigned are summarized in Tables I–III.

For states for which we have assigned $L=0$ values based on DWBA calculations, we have extracted enhancement factors ϵ given by the relation

$$\sigma_{\rm exp} = N\epsilon\sigma_{\rm DW} \ , \qquad (1)$$

where $\sigma_{\rm exp}(\sigma_{\rm DW})$ is the experimental (DW calculated) cross section, and $N=22$ is the normalization factor obtained from a systematic comparison[19] between empirical and DW calculated (t,p) strengths. The enhancement factors are summarized in Table VI and it is these numbers, which are independent of mass and Q-value effects, that will be used in comparing the observed (t,p) strengths to the predictions of the IBA and other models.

IV. DISCUSSION

A. Energy systematics

The systematics of the low-lying low spin states in $^{186-200}$Pt are summarized in Fig. 7. The figure includes our present study of ^{200}Pt as well as level information taken from the literature. Upon cursory examination of Fig. 7 one notices the monotonic rise in the energy of the 2_1^+ state, which is tracked by the energy of the 4_1^+ state, and the nonmonotonic behavior of the energy of the first excited 0^+ state.

To examine the energy trends in more detail, we have plotted several energy ratios and differences in Fig. 8. In Fig. 8(a) we illustrate the difference $\Delta E(2_1^+)$ in the energies of the 2_1^+ states in neighboring even Pt isotopes. This quantity gives an indication as to how fast the structure is changing from nucleus to nucleus. The structure of $^{188-196}$Pt is fairly similar, as evidenced by the relatively small (~25 keV) values of $\Delta E(2_1^+)$, while the change in structure between ^{196}Pt-^{198}Pt and ^{198}Pt-^{200}Pt is more dramatic, with $\Delta E(2_1^+)$ ~ 60 keV. The increasing 2_1^+ state energies indicate that, while $^{188-196}$Pt are fairly similar in structure, the trend toward a more spherical shape is quite evident for ^{198,200}Pt.

Another indication that the heavier Pt isotopes are more spherical than the $^{188-196}$Pt nuclei is the energy ratio of the 4_1^+ state to the 2_1^+ state, as shown in Fig. 8(d). For orientation purposes the predicted values for three limiting symmetries are also indicated. For a rotor, which corresponds to the SU(3) limit[2] of the IBA, this value should be 3.33; for the displaced γ-unstable vibrator, which corresponds to the O(6) limit[3] of the IBA, with degenerate 4_1^+ and 2_2^+ states, the value is 2.5; and for a harmonic vibrator, which corresponds to the O(5) limit[1] of the IBA, the value would be 2.0. As can be seen in Fig. 8(d), the value of $E(4_1^+)/E(2_1^+)$ is nearly constant at 2.5, although for ^{198}Pt and ^{200}Pt it is clearly tending towards the value of a harmonic vibrator, although that value is not attained.

Another energy quantity which is frequently a sensitive probe of nuclear structure is the energy difference between the 2_2^+ and 4_1^+ states. This energy difference has been recognized by Kumar[22] to be a measure of $V_{\rm PO}$, the difference in energy

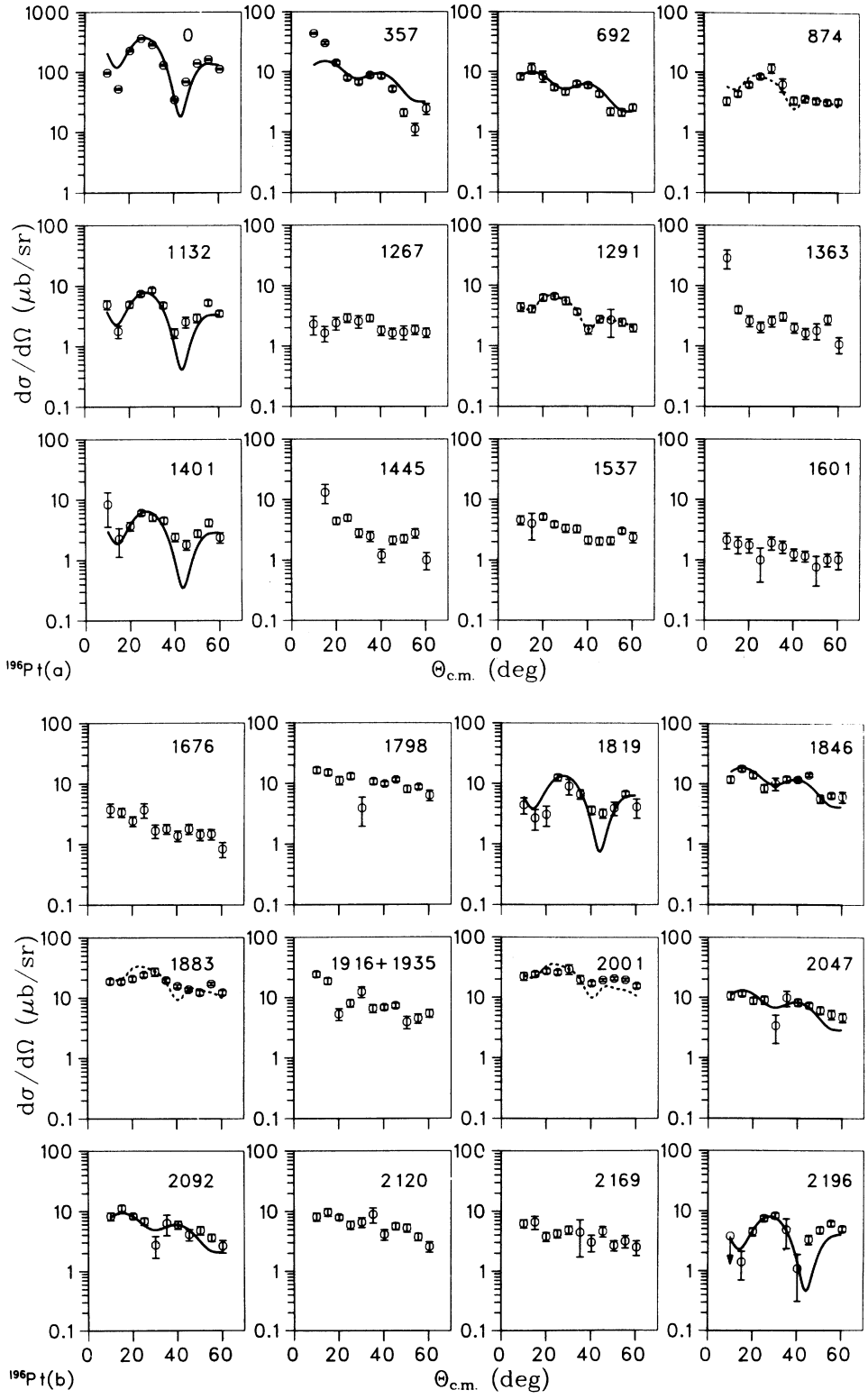

FIG. 4. Angular distributions measured for the ^{194}Pt$(t,p)^{196}$Pt reaction at $E_t = 17$ MeV. The states are labeled by their excitation energies in keV. Solid curves are DWBA calculations for $L = 0$ and $L = 2$ transfer. Dashed curves are empirical $L = 4$ angular distributions.

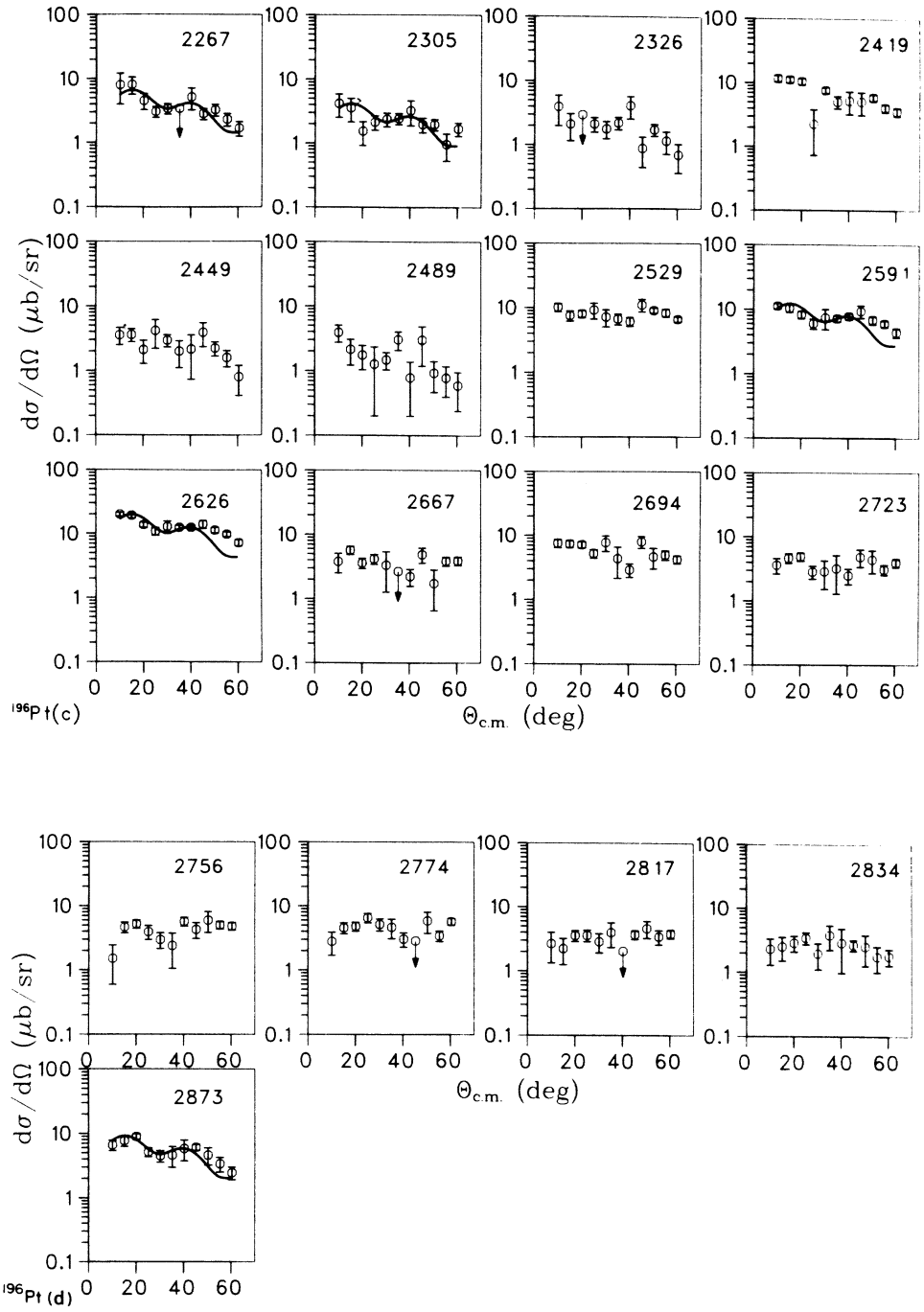

FIG. 4. (*Continued*).

between the prolate and oblate minima in the potential well describing the nucleus. If a nucleus is well deformed, V_{PO} is very large. However, for a spherical or γ-unstable nucleus V_{PO}, and hence $E(2_2^+) - E(4_1^+)$, should be very small. Given the trends toward a more spherical system indicated by Figs. 8(a) and 8(d), one would have expected Fig. 8(b) to show a tendency towards a *less*

TABLE II. States populated in ^{196}Pt(t,p) ^{198}Pt.

E_x (keV)[a] (t,p)	$d\sigma/d\Omega$ (μb/sr)[b] (25°)	L[c]	E_x (keV)[d] Ref. 15	J^π Ref. 15	E_x (keV)[e] $(n,n'\gamma)$	J^π $(n,n'\gamma)$
0	355(3)	0	0	0^+	0	0^+
408(5)	5.7(6)		407.2	2^+	407.0	2^+
780(5)	2.7(4)	(2)	775	(2^+)	774.5	2^+
			914.6	(0^+)	913.9	(0^+)
990(5)	13.8(8)	(4)	991	(4^+)	984.6	4^+
1291(5)	13.5(10)	(4)	1305			
1373(6)	1.6(3)				1366.7	(5^-)
1484(6)	5.3(5)	0				
1517(8)	0.4(3)					
1555(5)	3.6(5)	(2)				
1639(6)	5.5(9)	(2)				
1658(6)	12.1(12)					
1682(5)	5.8(8)					
1718(5)	11.4(10)	(2)	1722	(3^-)		
1779(5)	3.6(4)					
1815(6)	2.3(6)					
1869(5)	9.2(12)	0				
1892(5)	28(2)	(4)				
1938(6)	5.5(6)					
1956(6)	10.7(7)	(2)				
1977(6)	2.7(4)					
2059(6)	4.2(5)					
2083(7)	4.6(6)	(4)				
2119(6)	5.0(6)	(2)				
2149(6)	8.2(12)	(4)				
2170(6)	2.8(5)	(2)				
2229(6)	3.0(4)	(2)				
2252(7)	0.4(3)					
2289(6)	6.8(9)	(4)				
2325(6)	4.1(7)	(2)				
2352(6)	5.4(5)	(2)				
2373(7)	3.4(3)					
2411(6)	6.1(8)	(2)				
2440(6)	8.7(10)					
2472(6)	9.3(10)					
2531(6)	5.7(11)					
2574(6)	13(2)					
2628(6)	3.7(8)					
2683(6)[f]	6.2(8)					
2740(7)	9.9(9)					
2778(6)	7.3(9)					
2802(7)	4.5(7)	0				

[a] Excitation energy in keV measured in the present (t,p) study. Errors in parentheses are on the last digit(s).

[b] Cross section at 25° in μb/sr. Errors in parentheses reflect only relative errors on the last digit(s). There is an additional 15% error in determining absolute cross sections.

[c] Transferred L value determined in (t,p) investigation.

[d] Excitation energy in keV and J^π values as compiled in Ref. 15.

[e] Excitation energy in keV and J^π values as determined in the concurrent $(n,n'\gamma)$ study of Ref. 11.

[f] The 2683 keV transition is probably a doublet.

negative value of $E(2_2^+) - E(4_1^+)$ for $^{198,\,200}$Pt. However, this quantity is *more* negative.

It has recently been shown[23] that $^{188-196}$Pt could be well described within the IBA phenomenology as nuclei near the O(6) limit of that model. The O(6) limit had been suggested in Refs. 4 and 23 to be very similar to a γ-unstable vibrator; this correspondence has been verified in Ref. 24.

TABLE III. States populated in ^{198}Pt(t,p) ^{200}Pt.

E_x (keV)[a]	$d\sigma/d\Omega$ (μb/sr)[b] (25°)	L[c]	J^π
0	342(14)	0	0^+
466(6)	6.7(11)		(2^+)
863(6)	3.5(7)	(2)	(2^+)
1099(6)	16.8(13)	(4)	(4^+)
1263(5)	24(2)	(4)	(4^+)
1561(7)	2.2(8)		
1579(6)	5.1(8)	0	0^+
1617(8)	1.6(8)		
1684(9)	1.5(8)		
1726(6)	5.3(11)	(2)	(2^+)
1757(5)	7.9(12)	(2)	(2^+)
1842(7)	3.7(9)	(2)	(2^+)
1872(5)	3.9(9)		
1915(5)	4.2(9)		
1936(5)	13.9(15)	(4)	(4^+)
1986(5)	6.3(10)	(2)	(2^+)
2014(6)	7.8(15)	0	0^+
2118(7)	6.4(10)	(2)	(2^+)
2128(7)	5.9(12)		
2144(6)	2.4(17)		
2156(6)	13(2)	(2)	(2^+)
2168(6)	6.0(10)		
2253(7)	6.7(10)	0	0^+
2299(7)	3.2(8)		
2402(9)	3.3(8)		
2431(7)	4.7(9)		
2461(8)	3.8(11)	(4)	(4^+)
2491(10)	0.8(7)		
2525(10)	1.9(8)		
2551(8)	7.1(13)		
2668(9)	17(2)	(2)	(2^+)
2709(9)	3.8(9)		
2731(11)	2.7(9)		

[a] Excitation energy in keV measured in the present (t,p) study. Errors in parentheses are on the last digit(s).

[b] Cross section at 25° in μb/sr. Errors in parentheses reflect only relative errors on the last digit(s). There is an additional 15% error in determining absolute cross sections.

[c] L values and J^π values determined from the present investigation.

Therefore, the potential surfaces of these nuclei would have minima for both prolate and oblate deformation, but the energy difference between these minima would be small. From the trend of $E(2_2^+) - E(4_1^+)$ in ^{198}Pt and ^{200}Pt it appears that the depth of the potential wells is getting smaller, and that the prolate minimum is shrinking faster relative to the oblate minimum. Hence, ^{198,200}Pt would have more oblate shapes than the lighter isotopes, although the deformations are quite small. This idea is supported by predictions of Gotz and co-workers[25] who calculated potential wells for ^{198,200}Pt where the nuclei have small oblate deformations. Also recent calculations[26] of Tamura and co-workers of ^{198}Pt support small oblate deformations for the heavier Pt nuclei.

B. $L = 4$ transitions

The information concerning $L = 4$ transitions in the Pt(t,p) measurements is summarized in Table VII. For the present discussion we will adopt the tentative L assignments of Tables I–III. In addition, we have tabulated the centroid of the $L = 4$ strength and the summed strength. The summed strength should only serve as an indication of the total strength, since many transitions cannot be assigned definite L values. However, since most of the strongly populated [$d\sigma/d\Omega(25°) \gtrsim 10$ μb/sr] states can be assigned tentative L values, Table VII does present an indication of the trends in $L = 4$ strength.

The $L = 4$ strength is primarily concentrated at ~1.7 MeV in ^{196}Pt, while in ^{200}Pt this strength is concentrated in the lowest two 4^+ states. For ^{198}Pt the situation is intermediate, with the first two 4^+ states receiving considerable strength together with a strongly populated state at 1892 keV.

In the Pt(p,t) reaction[14] to ^{196}Pt the 4_2^+ and 4_3^+ states at 1293 and 1884 keV, respectively, received sizable transfer strength. For ^{194}Pt the 4_2^+ state and several states at 2 MeV received considerable transfer strength, while in ^{192}Pt none of the $L = 4$ transitions were particularly strong.

Enhanced population of 4^+ states has also been observed in (p,t) reactions in the Pb-Hg region.[27] In particular the 4_2^+ state in ^{202}Hg and the 4_1^+ state in ^{204}Pb are populated with equal strength. The dominant configurations for $L = 4$ transfer strength are predicted by DWBA calculations to be $(3p_{3/2}, 2f_{5/2})$ and $(3p_{1/2}, 2f_{7/2})$. The enhanced population of the 4_2^+ state in the ^{204}Hg(p,t) reaction has been interpreted[28] as due to the importance of the $p_{1/2}$ orbital in the heavier Hg isotopes; the depletion of the $p_{1/2}$ strength in the lighter Hg isotopes would predict less $L = 4$ strength. In a simple vibrational model, the population of the 4_2^+ state would be a forbidden three-phonon excitation.

This same mechanism could be responsible for the pattern of $L = 4$ strength observed in the Pt(t,p) and (p,t) reactions. In the lighter isotopes the $p_{1/2}$ strength is quite high lying and possibly fragmented by other interactions, so little $L = 4$ strength is observed at low excitation. In $^{194-196}$Pt the $p_{1/2}$ strength becomes lower in excitation, so that considerable $L = 4$ transfer strength is observed near 1700–2000 keV in excitation. Intermediate between $^{194-196}$Pt and ^{200}Pt

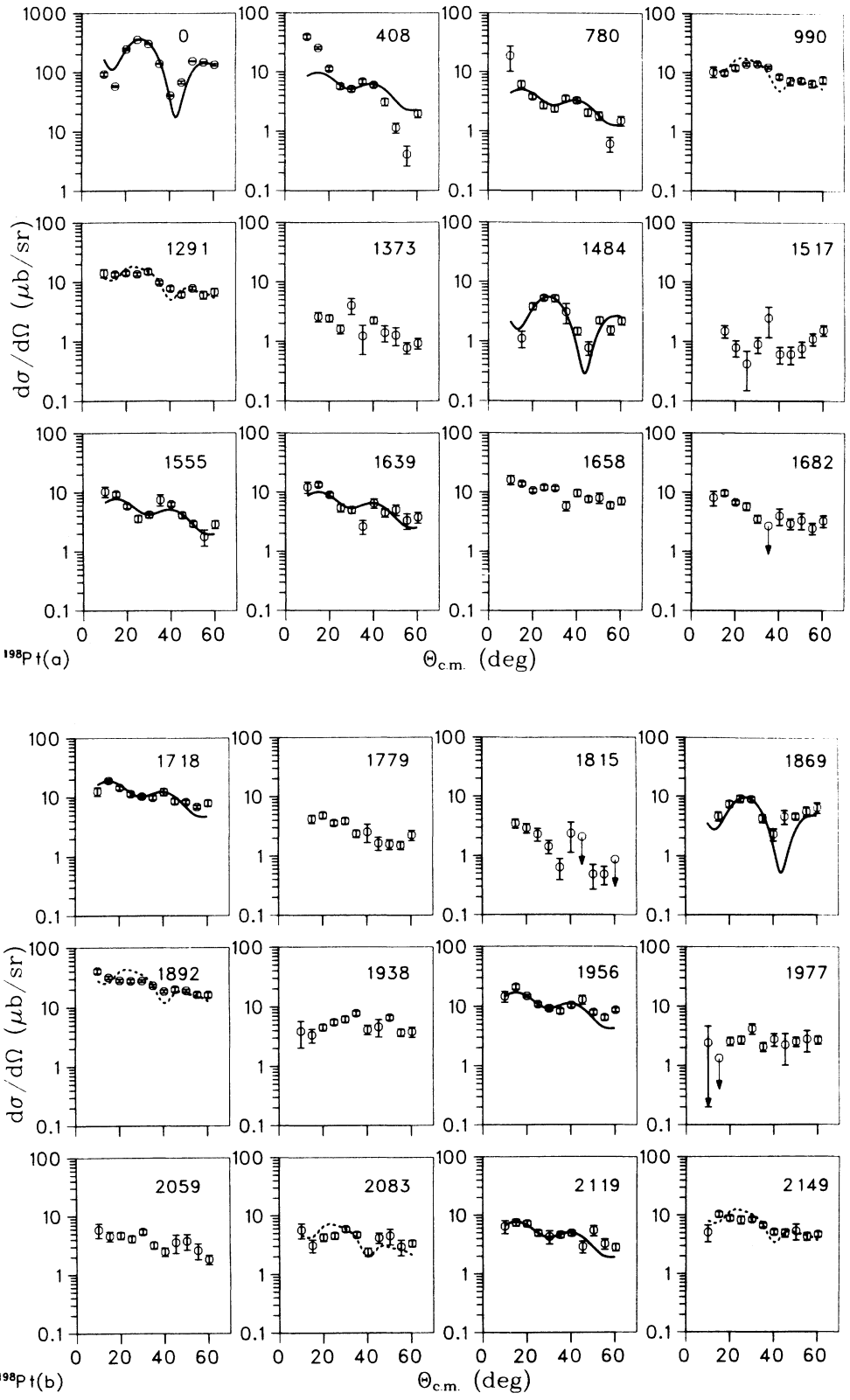

FIG. 5. Angular distributions measured for the ^{196}Pt$(t,p)^{198}$Pt reaction. See caption to Fig. 4.

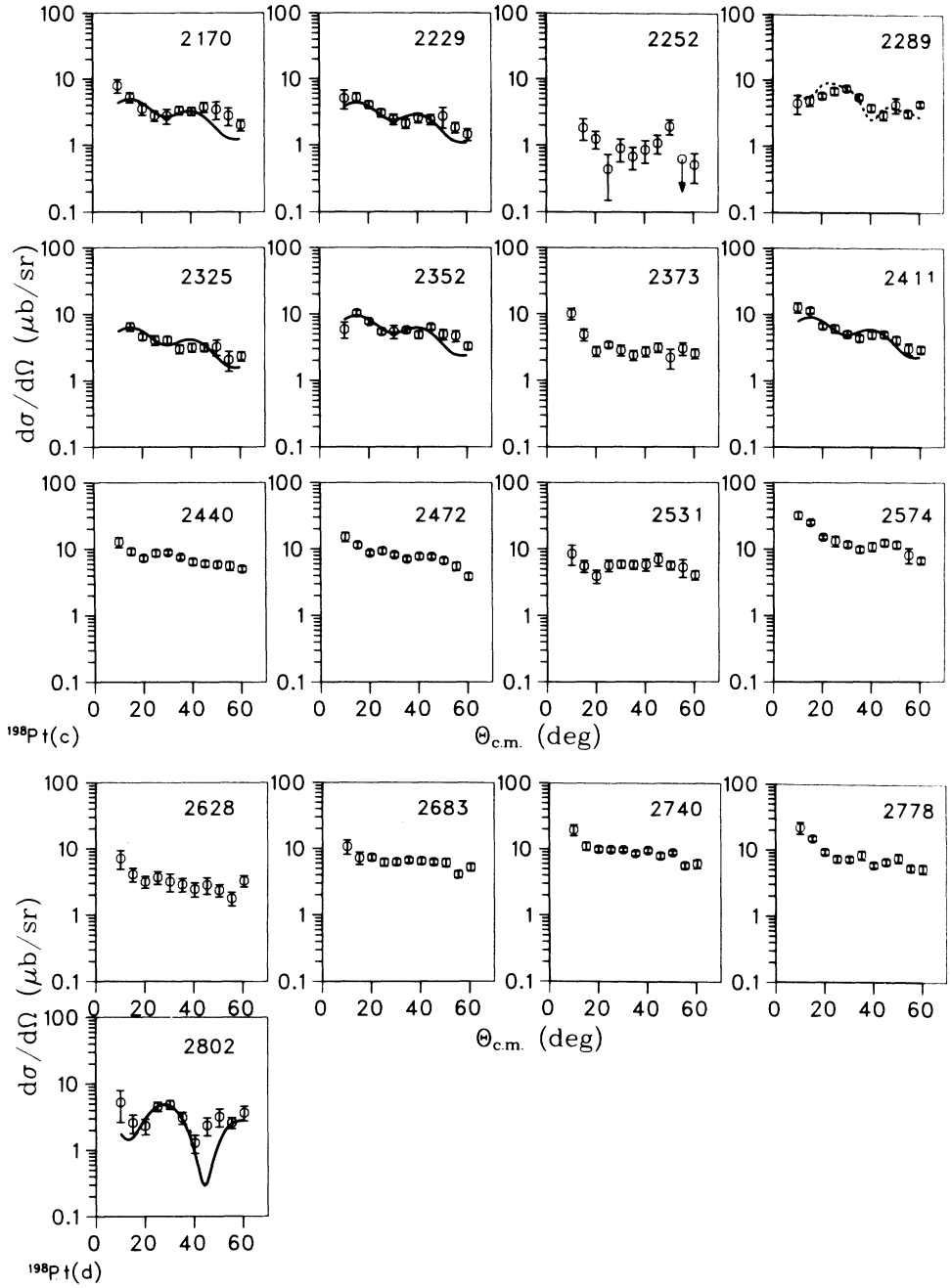

FIG. 5. (*Continued*).

would be ^{198}Pt where the $p_{1/2}$ strength has come low enough to enhance the $L=4$ transitions to the 4_1^+ and 4_2^+ states.

C. Interacting boson approximation model

The interacting boson approximation model[1-3] (IBA) is a framework for understanding collective excitations in medium and heavy mass nuclei. Since the bosons of the model can be thought of as pairs of particles, neutrons, or protons, coupled to angular momentum zero (s bosons) and two (d bosons) one has an obvious model for trying to understand two-particle transfer strengths outside of closed shell nuclei.

The Pt nuclei have recently been well described[23]

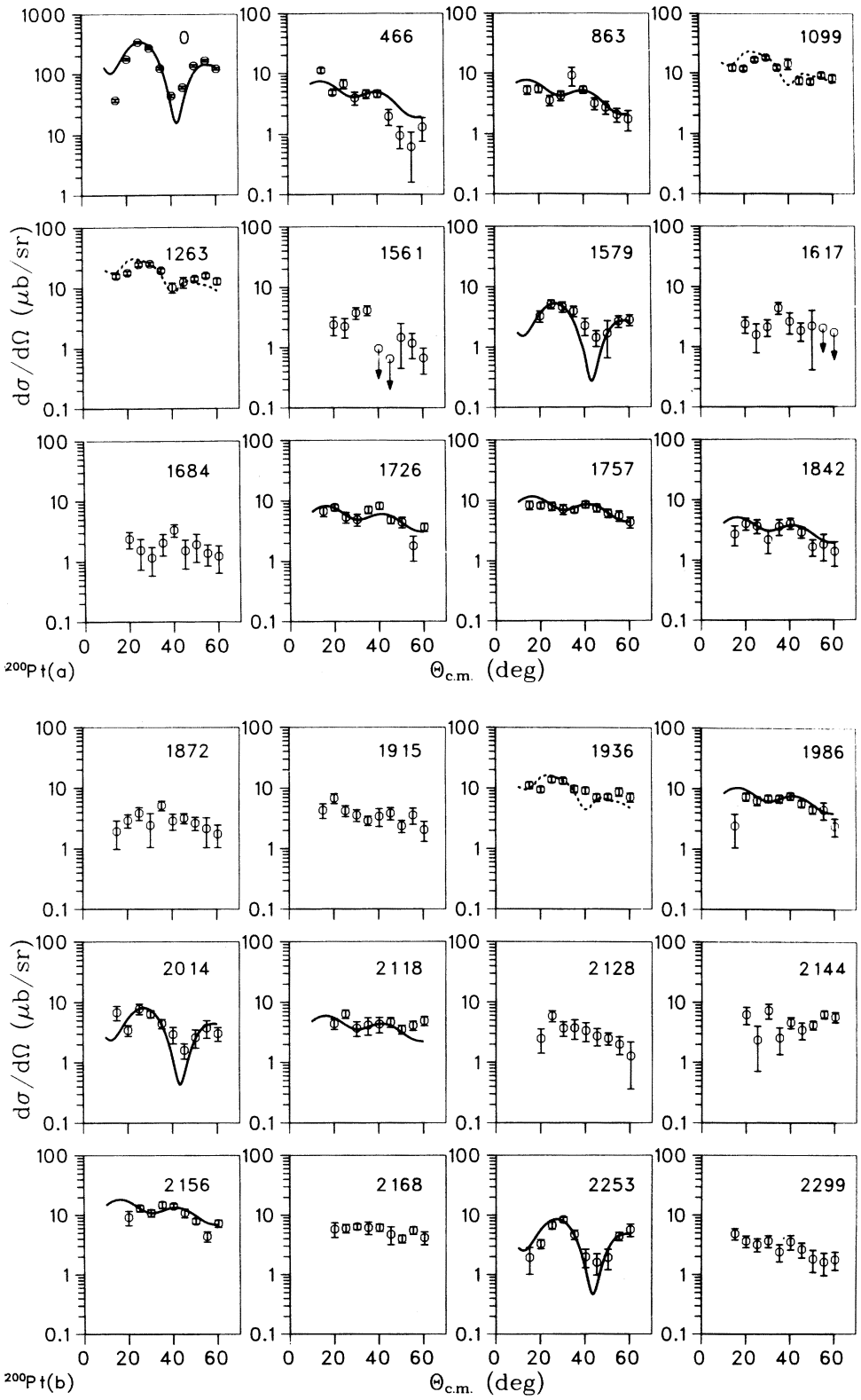

FIG. 6. Angular distributions measured for the ^{198}Pt(t,p)^{200}Pt reaction. See caption to Fig. 4.

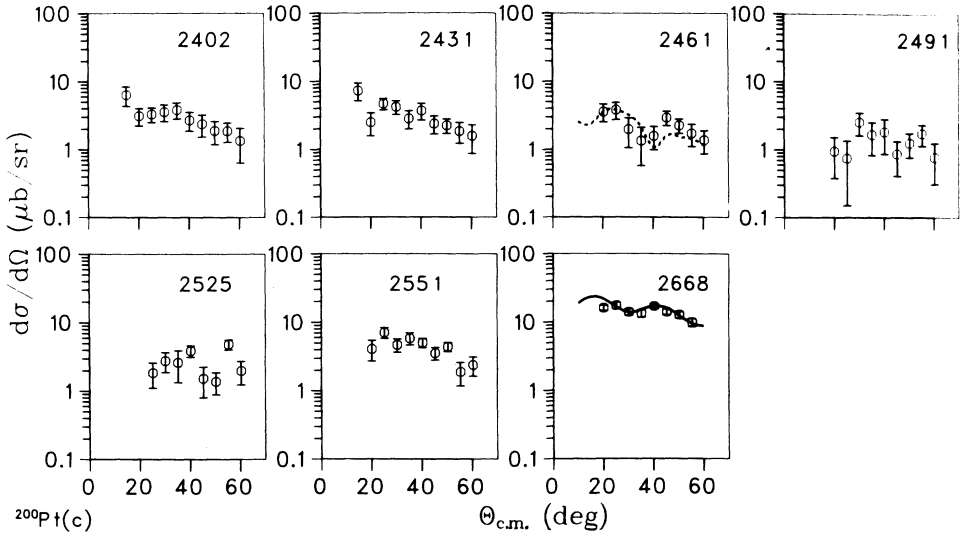

FIG. 6. (*Continued*).

as nuclei near the O(6) limit[3] of the IBA. The O(6) limit is very similar to the γ-unstable rotor of Wilets and Jean, in that there are, for example, a low-lying 2_2^+ state and a "missing" 0^+ state of the two-phonon triplet. The eigenvalues for all collective positive-parity states in an O(6) nucleus are given by[3]

$$E(\sigma, \tau, \nu_\Delta) = \frac{A}{4}(N-\sigma)(N+\sigma+4) + B\tau(\tau+3) + CJ(J+1), \quad (2)$$

where A, B, and C are constants, N is the total number of bosons (given by one-half the number of the valence protons and neutrons; for ^{196}Pt, $N=6$) and σ, τ, and ν_Δ are quantum numbers for distinguishing the different states. The range of values of σ, τ, and ν_Δ have been given in Refs. 4, 8 and 24.

In the O(6) limit there are simple selection rules for transitions. Gamma-ray $E2$ transitions follow the selection rule[3] $\Delta\sigma = 0$, $\Delta\tau = \pm 1$. Two particle transfer $L=0$ transitions follow the selection rule[5] $\Delta\tau = 0$, $\Delta\sigma = \pm 1$. In an O(6) nucleus one has two kinds of excited 0^+ states. The first has $\sigma = \sigma_{max} = N$ and large τ values; for example, the 0^+ state with quantum numbers $(\sigma, \tau\nu_\Delta) = (N, 31)$ which would correspond to a three-phonon 0^+ state in a spherical nucleus or a two-phonon γ-vibration in a deformed nucleus. The other has $\sigma < \sigma_{max}$ and $\tau = 0$; for example, the $(N-2, 00)$ 0^+ state. By examining the quantum numbers one can immediately determine how that state will decay or whether it should be strongly populated in a (t,p) reaction.

In ^{196}Pt three excited 0^+ states had been identified[14] prior to the present study. All of these states could be understood[4,8] within the framework of the O(6) limit of the IBA. The present work identifies two more 0^+ states. These states had been observed in an earlier (n,γ) study,[8] al-

TABLE IV. Ground-state transitions in ^{nat}Pt, Os(t,p) measurements.[a]

Target	$\frac{d\sigma}{d\Omega}(25°)$[b] μb/sr	$\frac{d\sigma}{d\Omega}$(rel)[c]	ϵ[d]	ϵ_{rel}[e]
^{198}Pt	300(20)	0.88(5)	10.1	0.75(5)
^{196}Pt	354(9)	0.97(4)	11.8	0.89(4)
^{194}Pt	366(7)	≡1.00(4)	12.7	≡1.00(4)
^{192}Pt	398(105)	0.92(12)	14.3	1.00(13)
^{192}Os	275(9)	≡1.00(5)	9.0	0.93(5)
^{190}Os	284(8)	1.00(5)	10.1	≡1.00(5)
^{188}Os	289(14)	0.94(7)	10.6	1.03(7)
^{186}Os	251(39)	0.84(8)	9.7	1.02(9)

[a] This table is very similar to Table I in Ref. 5. For more specific information, please refer to the earlier reference.

[b] Absolute cross sections at 25° in μb/sr. The errors quoted in parentheses on the last digit(s) are statistical only; there is an additional 15% systematic error.

[c] Relative cross sections normalized for Pt and Os separately from a weighted average of the relative cross sections measured at 25°, 30°, and 50°.

[d] Enhancement factors obtained from Eq. (1) with a $(2p_{3/2})^2$ form factor.

[e] Relative enhancement factors normalized to the ^{194}Pt$(t,p)^{196}$Pt and ^{190}Os$(t,p)^{192}$Os reactions for Pt and Os, respectively. As discussed in Ref. 5, these are not simple normalizations of values in column 4.

TABLE V. Optical model parameters used in (t,p) DWBA calculations.[a]

Particle	V (MeV)	r_r (fm)	a_r (fm)	W (MeV)	W_D (MeV)	r_W (fm)	a (fm)	V_{so} (MeV)	r_{so} (fm)	a_{so} (fm)	Ref.
t	166.7	1.16	0.752	10.5	0	1.498	0.817				17
p	51.2	1.25	0.650	0	13.5	1.25	0.47	7.5	1.25	0.47	18

[a] The values given are for the ^{198}Pt$(t,p)^{200}$Pt case. For the other Pt and Os targets, the parameters were modified according to the relations given in Refs. 17 and 18.

though not uniquely recognized as 0^+ states. In Fig. 9 we present the decay of the known five excited 0^+ states in ^{196}Pt. The upper numbers on the transition arrows are the experimental[8] relative $B(E2)$ transition strengths, assuming $E2$ transitions. These values are compared with the predictions of the IBA (lower numbers on transition arrows) with the assignments of states based on the same parameters as used in Ref. 8, that is, $A = 186$ keV, $B = 43$ keV, $C = 19$ keV in Eq. (2).

Due to the selection rule $\Delta\sigma = 0$ in the O(6) limit of the IBA, 0^+ states with $\sigma < \sigma_{max}$ are not permitted to decay to the lower 2^+ states with $\sigma = \sigma_{max}$. However, if the O(6) symmetry is broken slightly by changing the boson energy without introducing an additional boson-boson interaction, the σ selection rule is broken while the $\Delta\tau = \pm 1$ selection rule is preserved. Therefore, we have indicated in Fig. 9 how the excited 0^+ states would decay in this slightly broken O(6) scheme.

In the original (n,γ) study[8] the 0^+ states with quantum numbers (631), (400), and (200) had been identified; the present work identifies candidates for the (431) and (000) states. If the $\Delta\tau = \pm 1$ selection rule is preserved, one expects the 0^+ (431) state to predominantly decay to the 2_2^+ state, as is observed for the 2199-keV state, and the 0^+ (000) state to predominantly decay to the 2_1^+ state, as is observed for the 1918-keV state. These expected decay properties of 0^+ states were used in identifying the correspondence between the empirical and O(6) predicted levels. As has been pointed out in earlier examinations[4, 8, 23] of ^{196}Pt, the agreement between the empirical and O(6) limit predicted energies is quite poor.

Alternative assignments of these states are possible. The 2199-keV level, given that it decays predominantly to the 2_2^+ state, is probably a collective excitation. However, this state could also be assigned as the 0^+ (662) state, since one would expect that state to decay preferentially to the 2_2^+ (620) state, since that decay route is less forbidden than the decay to the 2_1^+(610) state. The (662) state is predicted from Eq. (2) to be higher lying than the (431) state, so the (431) assignment is preferred. The 1918-keV level could be a noncollective state, since it does decay predominantly to the 2_1^+ state and is above the pairing gap energy[8] of ~ 1.8 MeV. However, the decay pattern of this state does not contradict a collective character, and hence the assignment as the (000) state predicted by the IBA, is also valid.

The selection rules for two-neutron transfer reactions are $\Delta\sigma = \pm 1$, $\Delta\tau = 0$. For the target nucleus, the ground state has quantum numbers $(N, 00)$. The selection rules imply that the ground states of nuclei with $(N-1,00)$ and $(N+1, 00)$ will be populated in two-neutron transfer, and one excited 0^+ state with $(N-1, 00)$ in the nucleus with $N+1$ bosons will also be populated. In the Pt nuclei where the bosons are "holes," one therefore expects excited 0^+ states to be populated in only the (p,t) reaction and not the (t,p) reaction. The ground states should be strongly populated in both reactions.

A more quantitative prediction of two-neutron transfer strengths is also possible. In an O(6) nucleus, ground-state to ground-state transition strengths are given by[3]

$$I^{O(6)}(N \to N+1) \approx \alpha_\nu{}^2 \frac{(N+4)(N_\nu+1)}{2(N+2)} \times \left(\Omega_\nu - N_\nu - \frac{(N-1)N_\nu}{2(N+1)}\right), \quad (3)$$

where N is the total number of bosons, N_ν the number of neutron bosons, and Ω_ν the boson degeneracy of the neutron shell (for the 82–126 shell, $\Omega_\nu = 22$). Similar analytical expressions[29] for ground state transition strengths in the SU(5) and SU(3) limiting symmetries of the IBA exist. In Ref. 5, we compared the empirical relative ground-state transition strengths for Pt and Os to the strengths predicted by the three limiting symmetries of the IBA and found good agreement with the predictions of the O(6) limit. The SU(5) predictions deviated markedly from the observed strengths. Unfortunately, the SU(3) predictions of relative strengths were essentially indistinguishable from the O(6) values. However, there is considerable experimental evidence that these

TABLE VI. Comparison of empirical two-neutron transfer strengths with the predictions of the IBA.

Reaction[a]	E_x[b] (keV)	ϵ (exp)[c]	ϵ_{rel} (exp)[d]	IBA[e] J^π	A	B	O(6)
^{198}Pt(t,p)^{200}Pt	0	10.1	0.80	0_1^+	0.75	0.75	0.75
17 MeV	1579	0.20	0.02	0_2^+	0.0001	0.0056	
	2014	0.30	0.02	0_3^+	0	0	
	2253	0.36	0.03	0_4^+	0	0	
^{196}Pt(t,p)^{198}Pt	0	11.8	0.93	0_1^+	0.89	0.89	0.89
17 MeV	914	0.22	0.02	0_2^+	0	0	
	1484	0.39	0.03	0_3^+	0.0003	0.0004	
	1869	0.23	0.02	0_4^+	0	0.0001	
	2802	0.23	0.02				
^{194}Pt(t,p)^{196}Pt	0	12.7	≡1.00	0_1^+	≡1.00		≡1.00
17 MeV	1132	0.35	0.03	0_2^+	0		
	1401	0.25	0.02	0_3^+	0.0007		
	1819	0.56	0.04	0_4^+	0		
	1916	0.27	0.02				
	2196	0.38	0.03				
^{192}Pt(t,p)^{194}Pt	0	14.3	1.13	0_1^+	1.07		1.08
17 MeV							
^{198}Pt(p,t)^{196}Pt	0	3.7	1.03	0_1^+	0.89	0.89	0.89
35 MeV	1135	0.11	0.031	0_2^+	0	0	
	1402	0.15	0.042	0_3^+	0.12	0.12	
	1824	0.32	0.089	0_4^+	0	0	
^{196}Pt(p,t)^{194}Pt	0	3.6	≡1.00	0_1^+	≡1.00		≡1.00
35 MeV	1267	0.08	0.022	0_2^+	0		
	1479	0.03	0.008	0_3^+	0.13		
	1547	0.26	0.072	0_4^+	0		
^{194}Pt(p,t)^{192}Pt	0	5.1	1.42	0_1^+	1.07		1.08
35 MeV	1195	0.07	0.019	0_2^+	0		
	1628	0.26	0.072	0_3^+	0.13		
				0_4^+	0		
^{192}Os(t,p)^{194}Os	0	9.43	0.99	0_1^+	0.95		0.93
15 MeV	696	0.56	0.059	0_2^+	0.0081		
	1540	0.65	0.068	0_3^+	0.0018		
	1835	1.18	0.12	0_4^+	0		
^{190}Os(t,p)^{192}Os	0	9.51	≡1.00	0_1^+	≡1.00		≡1.00
15 MeV	956	0.42	0.044	0_2^+	0.0039		
	1206	0.90	0.095	0_3^+	0.0006		
	1924	0.87	0.091	0_4^+	0.0001		
^{188}Os(t,p)^{190}Os	0	10.97	1.15	0_1^+	1.01		1.04
15 MeV	912	0.21	0.022	0_2^+	0.0032		
	1734	0.49	0.052	0_3^+	0		
	2451	1.52	0.16	0_4^+	0.0011		

TABLE VI. (*Continued*)

Reaction[a]	E_x[b] (keV)	ϵ (exp)[c]	ϵ_{rel} (exp)[d]	IBA[e] J^π	A	B	O(6)
^{186}Os$(t,p)^{188}$Os 17 MeV	0	9.7	1.02	0_1^+	0.98		1.04

[a] The ϵ values for the ^{194,196,198}Pt(t,p) measurements were determined from the present study on enriched Pt targets. The ^{192}Pt(t,p) ϵ value was determined from the ^{nat}Pt measurement (see Table IV). The Pt(p,t) ϵ values are those obtained in Ref. 14. (Note that there is a discrepancy between ϵ values and integrated cross sections quoted in Ref. 14.) The ^{190,192}Os(t,p) ϵ values were obtained using standard DWBA parameters and the measured cross sections of Ref. 9. The ^{186}Os(t,p) ϵ value was determined from the ^{nat}Os measurement (see Table IV).

[b] The excitation energy in keV of 0^+ states determined from Refs. 9 and 14, and the present study.

[c] The enhancement factor ϵ obtained from Eq. (1) using a $(2p_{3/2})^2$ form factor. Errors are ~15 to 20%.

[d] Relative ϵ values normalized to the ^{194,196}Pt and ^{190,192}Os g.s.-g.s. transitions for Pt and Os, respectively.

[e] Predictions of the IBA model of two-neutron transfer strengths. The calculated strengths are normalized to the empirical ^{194,196}Pt and ^{190,192}Os g.s. to g.s. ϵ values, for Pt and Os, respectively. The strength is listed for the four 0^+ states calculated by the code FTPT. As discussed in the text, strength to $0^{+\prime}$ states is fairly insensitive to the IBA predictions, so one cannot make an unambiguous correspondence between observed and theoretical 0^+ states. For the numerical calculations, parameter set A is essentially the parameters used in Ref. 23 (the solid curves in Fig. 10); parameter set B (dashed curves in Fig. 10) represent a more vibrational [but near O(6)] structure for ^{198,200}Pt. For reference, the analytical values for ground-state transitions from the O(6) limiting symmetry are also given.

nuclei, especially the stable Pt isotopes, are not good rotors,[23] so it is reasonable to restrict the discussion to near-O(6) shapes.

Table VI summarizes the enhancement factors of $L=0$ transitions extracted from (t,p) and (p,t) measurements on Pt and Os nuclei. The Pt(p,t) ϵ values are taken from Ref. 14. The Os(t,p) study of Ref. 9 did not extract enhancement factors. The ϵ values quoted in Table VI were derived from the data of Ref. 9 using the code DWUCK 4 and standard optical parameters. Although Os(p,t) measurements[30] do exist, these measurements were performed at energies of $E_p = 18$–19 MeV, and given the fairly large negative Q values for the (p,t) reaction, one is unable to obtain reliable ϵ values to compare with theoretical predictions.

To examine two-neutron transfer strengths away from the O(6) symmetry, we have used the parameters for $^{186-194}$Os and $^{192-196}$Pt derived in Ref. 23 as input to the IBA codes[31] PHINT and two-particle transfer code FTPT.

The code FTPT calculates the transition matrix elements between the initial and final nuclei for both (t,p) and (p,t) reactions. Determining the appropriate parameters for ^{198,200}Pt was more difficult since relatively little information is known about these nuclei except for their energy levels. Also Fig. 8 indicates that the structure is changing in going towards these heavier nuclides. Therefore, several parameter sets were investigated, as summarized in Fig. 10. As was the philosophy of Ref. 23, no fine tuning of parameters to maximize the energy fit was done.

In Table VI and Figs. 11 and 12, we have compared the measured two-neutron transfer ϵ values for Pt and Os to the predictions of the IBA using the parameters of Fig. 10. First, we examine the relative ϵ values for each element illustrated in Fig. 11. Since ^{194,196}Pt have been well established[23] as nuclei very near the O(6) limit of the IBA, we have normalized the theoretical calculations to the transitions between ^{194,196}Pt. One can see in Table VI and Fig. 11 that the O(6) predictions fit the data quite well. There is evidence that the ϵ values extracted in Ref. 14 for the ^{196}Pt$(p,t)^{194}$Pt measurement are low. If one chooses another target to normalize to (as was done in Ref. 5) the agreement between the O(6) predictions and the (p,t) data will be improved. The SU(5) predictions are normalized to the ^{198}Pt$(t,p)^{200}$Pt data point, the transition between the most likely vibrational nuclei, and clearly deviate markedly from the data. There is no difference between parameter sets A and B in the relative ϵ values predicted for ^{198,200}Pt. If one arbitrarily imposes

TABLE VII. $L=4$ transitions in Pt(t,p) and (p,t) reactions.

Reaction[a]	E_x[b] (keV)	$\frac{d\sigma}{d\Omega}$ (μb/sr)[c]	$\frac{\sigma}{\sigma_{g.s.}}$ (%)[d]	$\bar{E}_x$[e] (keV)	$\sum\left(\frac{d\sigma}{d\Omega}\right)^t$ (μb/sr)
^{198}Pt$(t,p)^{200}$Pt	1099	16.8	4.9	1349	49
17 MeV	1263	24	7.0		
	1872	3.9	1.1		
	2461	3.8	1.1		
^{196}Pt$(t,p)^{198}$Pt	990	13.8	3.9	1693	75
17 MeV	1291	13.5	3.8		
	1892	28	7.9		
	2083	4.6	1.3		
	2149	8.2	2.3		
	2289	6.8	1.9		
^{194}Pt$(t,p)^{196}$Pt	874	8.5	2.3	1738	65
17 MeV	1291	6.6	1.8		
	1883	24	6.6		
	2001	26	7.2		
^{198}Pt$(p,t)^{196}$Pt	877	13	1.5	1660	172
35 MeV	1293	43	5.0		
	1884	116	13.6		
^{196}Pt$(p,t)^{194}$Pt	811	9	1.1	2002	231
35 MeV	1229	30	3.7		
	1911	71	8.9		
	2125	37	4.6		
	2246	18	2.2		
	2353	37	4.6		
	2638	29	3.6		
^{194}Pt$(p,t)^{192}$Pt	785	15	1.5	1245	42
35 MeV	1201	16	1.6		
	1937	11	1.1		

[a] The (t,p) measurements are taken from the present study; the (p,t) measurements are from Ref. 14.

[b] The excitation energy in keV of tentative and definite 4^+ states in Pt nuclei.

[c] The differential cross sections in μb/sr at 25° for the (t,p) study and 7° for the (p,t) study.

[d] Cross sections of 4^+ states relative to the ground-state transition of that reaction.

[e] Centroid energy of $L=4$ strength in the particular reaction.

[f] Summed $L=4$ strength. See text for further discussion.

a purely vibrational structure on ^{198}Pt and/or ^{200}Pt, there is a significant decrease in the IBA-predicted (t,p) strengths. Qualitatively, one would expect that the overlap of ground-state wave functions between a γ-unstable nucleus and a vibrational nucleus would not be as large as between two γ-unstable nuclei. The IBA provides a quantitative measure that the heavier Pt isotopes are *not* good vibrators, but rather very similar in structure to the $^{192-196}$Pt nuclei.

If one looks only at relative ϵ values, Fig. 11 shows that the (t,p) ground-state (g.s.) strengths of the Os nuclei are fairly insensitive to the underlying structure since O(6), SU(3), and the intermediate calculation[23] all reproduce the data fairly well.

The two-neutron transfer strengths to excited 0^+ states are not a sensitive probe of the structure, as seen in Table VI and Fig. 11. Transitions to 0^+ states that are forbidden in the IBA framework are observed with 2–3% of the ground-state transition strength, presumably due to two-quasiparticle admixtures in the wave functions. Since allowed transitions are predicted to be ~8% of the ground state strength, the differences between allowed and forbidden transitions to excited 0^+ states is not as dramatic as the differences in the γ-ray decay properties of these states.[4,23]

If one carefully accounts for the Q value and A dependences in measured (t,p) cross sections, as was done for the Pt, Os(t,p) ϵ values extracted

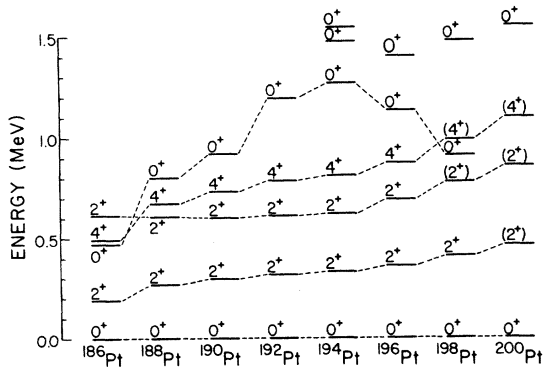

FIG. 7. Energy systematics of low-lying 0^+, 2^+, and 4^+ states in the Pt nuclei. The data are taken from Refs. 8, 14, 15, 20, 21, and the present study.

in Table IV, one can compare (t,p) strengths between elements, as illustrated in Fig. 12. These experimental values were obtained from natural targets in the identical experimental setup and should have relative accuracies of at least ±5%. By normalizing the O(6) limit predictions to the measured ^{194}Pt$(t,p)^{196}$Pt ϵ value, one has effectively determined the α_ν coupling factor in Eq. (3) and can compare predictions of (t,p) strengths to different symmetries. One finds that the measured Os(t,p) strengths are intermediate between the predictions for the O(6) and SU(3) limiting symmetries of the IBA. However, using the parameters of Ref. 23, one cannot reproduce the measured (t,p) strengths. This discrepancy may be due to the simplicity of the IBA model used in the present study, where we have assumed that α_ν does not depend on the number of proton bosons.

Within the framework of the IBA, there have been recent attempts[32,33] to understand the structure of nuclei by explicitly accounting for the neutron and proton degrees of freedom. The two-boson IBA-2 model predictions of Bijker and coworkers are shown in Fig. 12. These calculations do reproduce the observed ϵ values in Pt, but

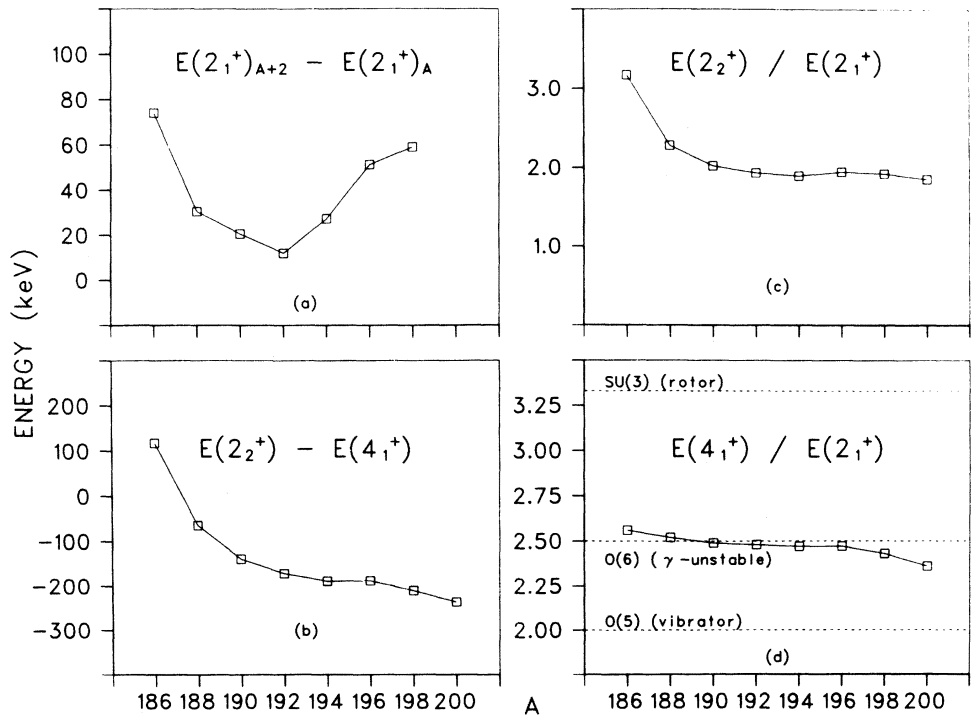

FIG. 8. The systematics in the Pt isotopes of several energy quantities. Part (a) is the difference in energy of the 2_1^+ states in neighboring Pt nuclei plotted as a function of A. Part (b) is the difference between the energy of the 2_2^+ and 4_1^+ states in keV. Part (c) is the ratio of the 2_2^+ and 2_1^+ state energies. Part (d) shows the ratio of the 4_1^+ and 2_1^+ state energies. The dashed lines give the predicted ratios for three limiting symmetries of the IBA. The data are taken from Refs. 8, 15, 20, and the present study.

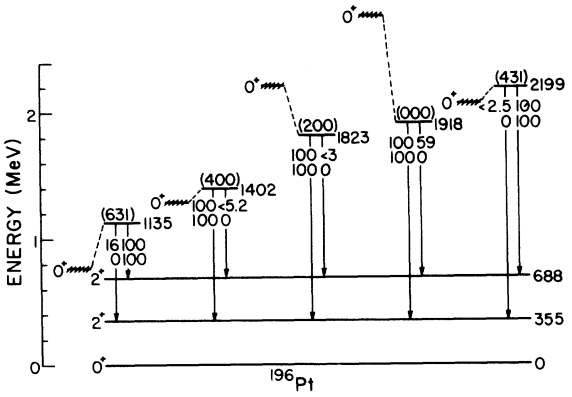

FIG. 9. The decay patterns of excited 0^+ states in ^{196}Pt. The states are labeled by their excitation energies in keV determined in the (n,γ) study of Ref. 8 and by the O(6) quantum numbers $(\sigma\tau\nu_\Delta)$. The cross-hatched lines are at the values predicted by the O(6) limiting symmetry of the IBA from Eq. (2) using $A=186$ keV, $B=43$ keV, and $C=19$ keV. The numbers on the transition arrows are the empirical (upper) and O(6) limit predicted (lower) relative $B(E2)$ values, assuming the transitions to be pure $E2$. The data are taken from Ref. 8. The IBA predictions and level assignments are discussed further in the text.

predict stronger transitions for the Os nuclei than observed. This inadequacy of the IBA to reproduce two-neutron "absolute" strengths may be due to several effects. Possibly, the method used to extract the ϵ values really does not correspond to an absolute strength, and therefore, the comparison between Pt and Os in Fig. 12 is meaningless. If one assumes that the method is correct, then one is left with an inadequacy of the IBA model as investigated so far to understand two-particle transfer. It is well known that certain single-particle orbitals such as $p_{3/2}$ give large (t,p) and (p,t) strengths. If the relative location of the Fermi surfaces in Pt and Os are such that Pt is closer to the "hot orbitals" while Os is further away, one would expect the Pt ϵ values to be larger than those in Os. Since the IBA-1 and IBA-2 models only deal with the collectivity of the ground-state wave functions and so far one does not have the specific single particle components of the bosons, maybe it is unrealistic to expect the IBA to reproduce all trends in two-neutron transfer strengths. However, the success the IBA has in reproducing relative ϵ values, especially in Pt, may indicate that the importance of particular orbitals is less critical for a given isotope chain and, therefore, it is valid to compare IBA predictions to relative ϵ values for each element.

D. Schematic models

Recently, Ginocchio has considered schematic shell model Hamiltonians[34] which have a class of eigenstates made up of monopole and quadrupole pairs. The model is schematic because, unlike the case of real nuclei, the single particle energies are degenerate and only quadrupole-quadrupole and pairing nucleon-nucleon interactions are considered. However, with these limitations, the problem can be solved analytically using group theory for special cases. The approximations are assumed to be valid for heavy nuclei far from closed shells. Here two-nucleon interactions should dominate so that the single-particle energy spacings are less important. Also there has been considerable success in understanding the structure of heavy nuclei in many different kinds of approaches that only consider quadrupole-quadrupole and pairing interactions. The group symmetry for which the states consist of monopole and quadrupoles pairs is that of SO(8), the special orthogonal group in eight dimensions. There is a one-to-one correspondence[34] between the states of SO(8) symmetry, generated from fermions with no boson approximation, and those of the interacting boson approximation model of Arima and Iachello. In particular, the SO(6) limiting symmetry of the Ginocchio model is analogous to the O(6) symmetry of the IBA.

In calculating two-nucleon transfer strengths in the IBA,[29] a cutoff factor had to be introduced to account for the finite dimensionality of the valence shell and the Pauli exclusion principle that the fermions, the underlying structure of the bosons, would observe. Arima and Iachello used a Primakoff cutoff factor[35] to account for the Pauli principle. This is valid for a system where only s bosons are important, such as the SU(5) limit of the IBA, but in the O(6) limit the ground state wave function also has d-boson components, and it is not known whether or not the modified Primakoff factor used by Arima and Iachello [quoted in Eq. (3)] is the correct Pauli correction.

In the Ginocchio model, the Pauli exclusion is properly accounted for since it deals with fermion Hamiltonians. For the vibrational limit one obtains[34] for the transfer strength S:

$$S_\nu^{\mathrm{VIB}}(N_\nu \to N_\nu+1)=(N_\nu+1)(\Omega_\nu-N)\ , \tag{4}$$

and for the SO(6) limit:

$$S_\nu{}^6(N_\nu \to N_\nu+1)=\frac{(N+4)(N_\nu+1)}{2(N+2)}\ (\Omega_\nu-2N_\nu)\ , \tag{5}$$

where N, N_ν, and Ω_ν have the same meaning as

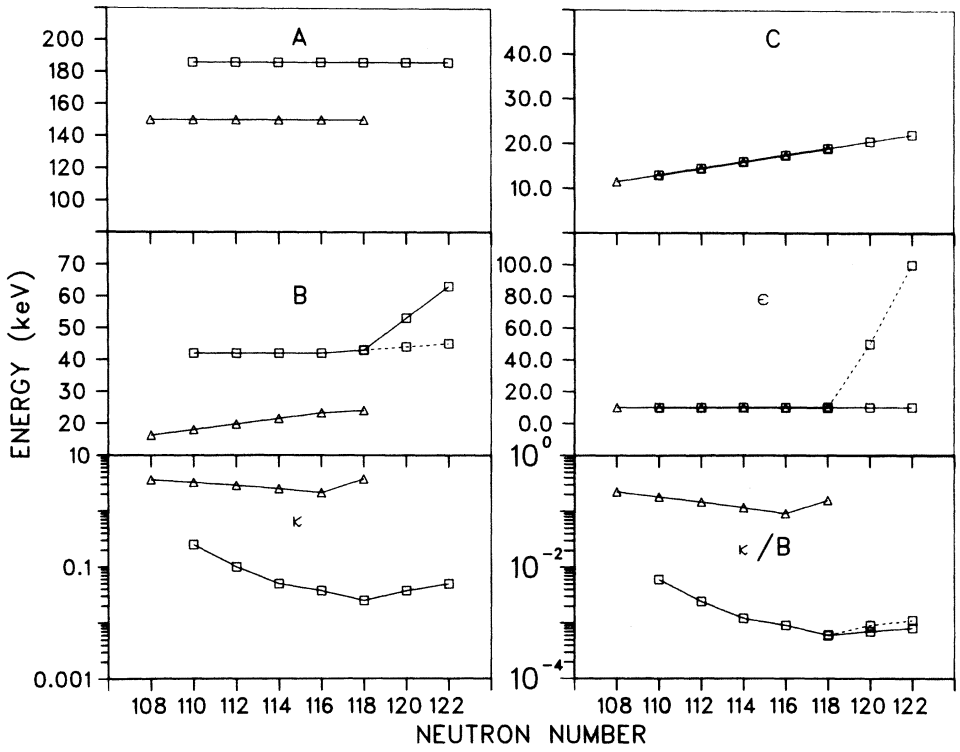

FIG. 10. Parameters for Pt (squares) and Os (triangles) used in the numerical IBA calculations discussed in the text. The solid lines are parameter set A; the dashed lines are parameter set B for ^{198,200}Pt. A, B, and C are the constants in Eq. (2). ϵ is the energy of the d boson, equal to zero in the pure O(6) limit and very large in the SU(5) limit. κ is the strength of the quadrupole-quadrupole interaction between d bosons. The ratio κ/B is a measure of the deviation of the structure from that of the O(6)-limiting symmetry. The parameter set A is essentially that of Ref. 23, where the importance of the various parameters is discussed in detail. See the text for discussion of parameters in relation to two-neutron transfer strengths.

in Eq. (3). The expression for the vibrational limit is the same as in the IBA, while for the SO(6) limit the cutoff factor is more dramatic. An analytical expression for transfer to excited 0^+ states also exists.

In Fig. 13, we present a comparison between the (t,p) strengths for the Pt targets and the predictions of Ginocchio's SO(6) limit. For reference, we have also plotted the predictions of the IBA O(6) symmetry. Both the schematic and IBA predictions reproduce the available data. The deviations between the models become quite drastic for large values of N. Also the schematic model predicts[34] very large transfer strengths to excited 0^+ states in (p,t) for large N. It would be very interesting to probe the SO(6) predictions for large values of N. Unfortunately, there are no examples of SO(6) [or O(6)] nuclei with large values of N that are sufficiently stable on which to perform (p,t) reactions.

E. Boson expansion technique

Kishimoto, Tamura, and Weeks have developed over several years a boson expansion model (BET) to understand the collective excitations in medium and heavy mass nuclei. Recently, Tamura and Weeks have applied the BET to the Pt-Os region.[26]

In the BET, the shell model Hamiltonian with monopole and quadrupole pairing and quadrupole-quadrupole interactions is expanded in terms of bosons up to sixth order. The single-particle energies are taken from empirical values for ^{207}Pb, except for the energy of the $i_{13/2}$ orbital which is made to vary smoothly as a function of mass. Additional parameters are f_2 and g_2, which are related to the strengths of the quadrupole pairing and quadrupole-quadrupole interactions, respectively, and are varied to fit the data, while retaining val-

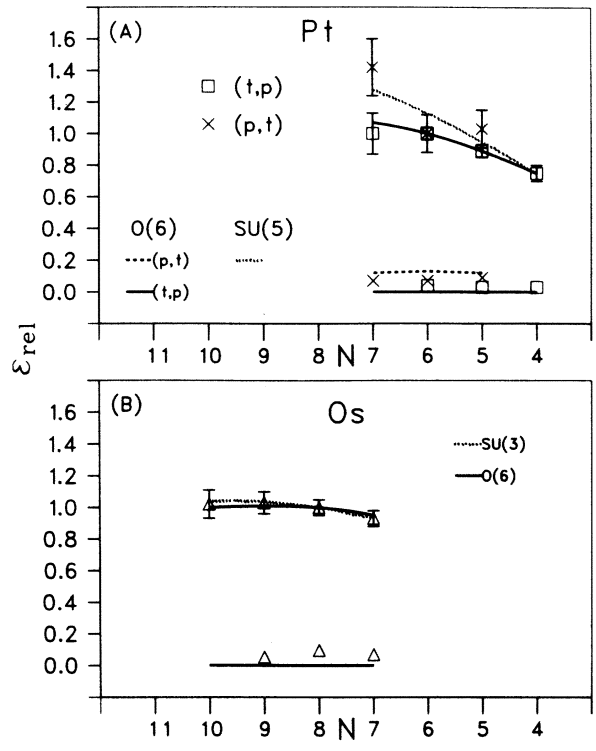

FIG. 11. Comparison of relative empirical and IBA-predicted two-neutron transfer strengths for Pt(t,p) (squares), Pt(p,t) (crosses), and Os(t,p) (triangles) measurements. In part (A) O(6) limit (t,p) (solid) and (p,t) (dashed) and SU(5) limit (dotted) predictions are shown for ground-state and allowed excited 0^+ transitions. The strengths ϵ are plotted as a function of the boson number N. For (t,p), N is that of the final nucleus; for (p,t), N is that of the target. The O(6) predictions are normalized for the ^{194,196}Pt g.s. transition; the SU(5) predictions are normalized for the ^{198,200}Pt g.s. transition. In part (B) the O(6) limit (solid) and SU(3) limit (dotted) predictions are shown for $L=0$ transitions in (t,p) as a function of N. The IBA predictions are normalized for the ^{190,192}Os g.s. transition.

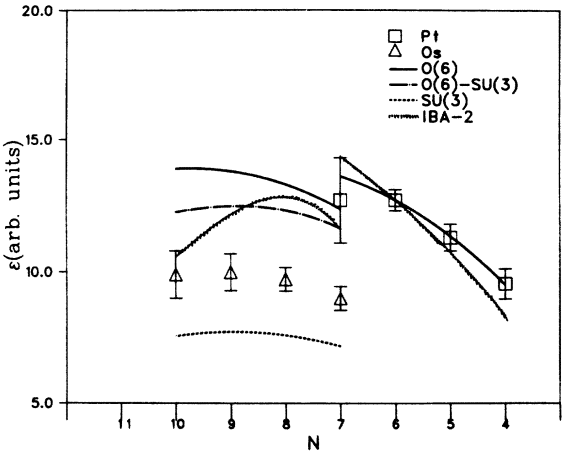

FIG. 12. Comparison of IBA-predicted (t,p) ground-state strengths and measured enhancement factors ϵ for Pt (squares) and Os (triangle) (t,p) reactions as a function of the boson number N of the final nucleus. The IBA predictions are shown for the O(6) limit (solid), SU(3) (dashed), and O(6) → SU(3) (dot-dashed) numerical calculations discussed in the text. The value of α_ν in Eq. (3) is determined by normalizing the O(6) prediction to the empirical value obtained in the ^{194}Pt$(t,p)^{196}$Pt reaction (^{194,196}Pt are examples of O(6) nuclei, as discussed in Ref. 23). IBA-2 calculations of Ref. 33 are indicated by the dotted line.

ues near microscopic ones.

To date, the energy levels and potential surfaces of $^{186-198}$Pt have been calculated. The BET is able to reproduce the energies in ^{198}Pt reasonably well, in particular reproducing the energy of the first and second excited 0^+ states (0_2^+ and 0_3^+). As mentioned earlier, the BET also predicts that the potential energy surface for ^{198}Pt gives a more oblate structure to this nucleus than to the lighter Pt nuclei, presumably because the prolate minimum of the γ-unstable shape is shrinking faster than the oblate minimum.

In the framework of the BET one is also able to calculate two-neutron transfer cross sections.[26] The BET two-neutron transfer calculations are essentially BCS calculations in which slight adjustments to the ground-state correlations induced by the quadrupole interaction are included. The spectroscopic amplitudes for each single particle configuration were calculated microscopically.

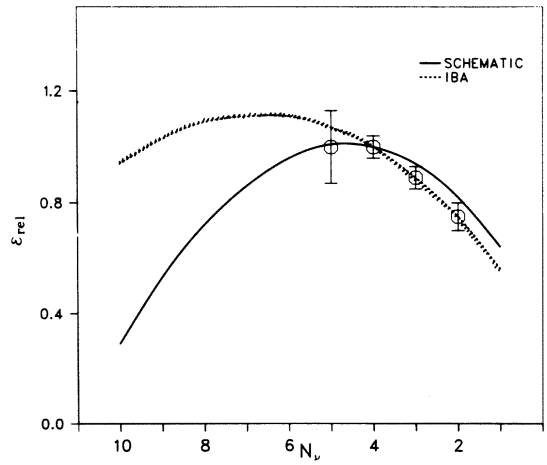

FIG. 13. Comparison of empirical and Ginocchio-model predicted Pt(t,p) strengths. The predictions of the SO(6) (solid) schematic model and the IBA O(6) (dashed) model are shown as a function of the boson number N_ν of the final nucleus. The calculations are normalized to the measured ^{194,196}Pt g.s. transition.

Cross sections were obtained[26] from the square of the form factor at the nuclear surface using a zero-range Bayman-Kallio method[36] for obtaining the form factor.

A comparison between the BET predictions and the empirical Pt(t,p) and (p,t) cross sections is summarized in Fig. 14. Although the BET does not exactly reproduce the (t,p) cross sections to ^{198}Pt, it fits the observed two-neutron transfer cross sections fairly well. A further test of the BET would be a comparison of Os(t,p) and Pt(t,p) strengths as was done in Fig. 12 for the IBA.

F. The pairing vibration model

The pairing vibration model[37] of Bohr and Mottelson has had considerable success in understanding two-neutron transfer strengths near closed shell nuclei. In the pairing vibrational picture the (t,p) ground-state strength will be proportional to the number of phonons, given by the number of neutron pairs away from the closed shell. For the Pt targets one would expect ratios of 0.6: 0.8: 1.0: 1.2 for 198:196:194:192 compared to the empirical values of 0.75: 0.89: 1.00: 1.00 taken from Table IV. Qualitatively, the simple pairing vibration trend is observed, but there is a marked deviation in the actual numbers, even greater than in the comparison of the Pt numbers to the SU(5) IBA predictions. The pairing rotation scheme, which may be appropriate for the mid-shell region, would predict equal ground-state transition strengths, as is observed for the Os nuclei. So, qualitatively, one may be observing a transition between the simple pairing vibrational and pairing rotational structures.

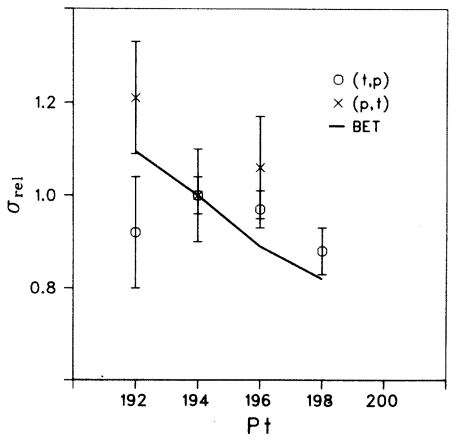

FIG. 14. Comparison of empirical and BET calculated Pt(t,p) (circles) and (p,t) (crosses) relative cross sections. The calculations are normalized to the measured ^{194,196}Pt g.s. transitions. The values are plotted as a function of target nucleus in (t,p) and the final nucleus for (p,t).

Another concept of the pairing vibration picture which may occur in Pt is the existence of a strong excited 0^+ state due to particles above the $N=126$ shell. Such a state is well established in the lead nuclei for both ^{206}Pb and ^{208}Pb. ^{200}Pt with only two fewer neutrons than ^{206}Pb should present definite possibilities for such states. Examination of the spectra up to 5.5 MeV showed no evidence for the existence of strongly excited 0^+ states, indicating that the expected strength is either at higher excitation or is considerably fragmented. There is also the possibility that the ^{198}Pt ground state is sufficiently deformed that there is only little overlap with the expected spherical excited 0^+ state. However, (^{3}He, n) studies on the Pt isotopes[38] do excite proton pairing vibrations of the expected strength and energy leading to the Hg isotopes. Thus, it is uncertain where this 0^+ strength lies. There is certainly no evidence for it in the 0^+ states up to 2.2 MeV as indicated in Table VI.

V. CONCLUSIONS

We have measured the (t,p) reaction on enriched ^{194,196,198}Pt targets. As a result, we have provided the initial study of excitations in ^{200}Pt and have identified two new 0^+ states in ^{196}Pt, three new 0^+ states in ^{198}Pt, and three 0^+ states in ^{200}Pt. The level structure of ^{198,200}Pt indicates that these nuclei are tending towards a more vibrational character than the lighter Pt nuclides, except that the overall shape may be more oblate rather than the γ-unstable shape of $^{192-196}$Pt. Systematics of the distribution of $L=4$ (t,p) and (p,t) strengths in the Pt nuclei can be understood qualitatively as resulting from the location of the $p_{1/2}$ shell model orbital with respect to the Fermi surface, the same mechanism that one obtains in the Hg region.

The ground-state to ground-state (t,p) spectroscopic strengths have been extracted and are found to vary smoothly over the targets studied, indicating an essentially stable structure for $^{192-200}$Pt. The interacting boson approximation model has been quite successful in understanding the trends in Pt and Os, although the IBA cannot reproduce the differences in strength between Pt and Os, possibly indicating a need for a more microscopic model. Unfortunately, the population of excited 0^+ states is not a sensitive test of the IBA predictions. Although the simple pairing vibration model qualitatively reproduces the trends in ground-state transition strengths, the excited $L=0$ strength expected above the $N=126$ shell is

not observed.

In addition to the IBA model, we have also looked at other more microscopic models and their predictions. The schematic model of Ginocchio predicts (t,p) strengths which are again in good agreement with the Pt(t,p) ground-state transition strengths. The Ginocchio model is actually a more microscopic derivation of the IBA and its predictions and, therefore, better reflects the fermion structure of the bosons. The boson expansion technique description has had success in understanding the level structure and the electromagnetic transitions in the Pt-Os nuclei. The present study shows that the BET also does reasonably well in understanding ground-state two-neutron transfer cross sections. What is rather surprising, and hopefully not fortuitous, is that the Pt(t,p) ground state transitions are best fit with the predictions of the O(6) limiting symmetry of the IBA. The O(6) limit predictions are also in good agreement with the electromagnetic properties of the Pt nuclei. This may be an indication that the O(6) symmetry is the dominant structure in Pt and one needs to understand further the microscopic basis of this symmetry, rather than a microscopic description of these nuclei that does not incorporate the symmetry concepts.

ACKNOWLEDGMENTS

We are very grateful to J. Gursky for fabricating the Pt and Os targets used in the present measurement and to the staff of the Van de Graaff Accelerator Facility for operation of the accelerator. We would also like to thank A. Arima, R. F. Casten, J. Ginocchio, and F. Iachello for highly stimulating and informative discussions; P. T. Deason, R. M. Ronningen, S. W. Yates, A. E. L. Dieperink, and K. J. Weeks for providing their results prior to publication; and O. Scholten for providing and discussing with us the IBA codes. This work was supported by the U. S. Department of Energy.

---

*Present address: A. W. Wright Nuclear Structure Laboratory, Yale University, New Haven, Conn. 06511.

†Present address: Sandia Laboratories, Albuquerque, New Mexico.

[1]A. Arima and F. Iachello, Ann. Phys. (N.Y.) 99, 253 (1976).

[2]A. Arima and F. Iachello, Ann. Phys. (N.Y.) 111, 201 (1978).

[3]A. Arima and F. Iachello, Ann. Phys. (N.Y.) 123, 468 (1979).

[4]J. A. Cizewski, R. F. Casten, G. J. Smith, M. L. Stelts, W. R. Kane, H. G. Börner, and W. F. Davidson, Phys. Rev. Lett. 40, 167 (1978).

[5]J. A. Cizewski, E. R. Flynn, R. E. Brown, and J. W. Sunier, Phys. Lett. 88B, 207 (1979); and references therein.

[6]E. R. Flynn, S. Orbesen, J. D. Sherman, J. W. Sunier, and R. Woods, Nucl. Instrum. Methods 128, 35 (1975).

[7]E. R. Flynn, Nucl. Instrum. Methods 162, 305 (1979) and references therein.

[8]J. A. Cizewski, R. F. Casten, G. J. Smith, M. R. Macphail, M. L. Stelts, W. R. Kane, H. G. Börner, and W. F. Davidson, Nucl. Phys. A323, 349 (1979); R. F. Casten, private communication.

[9]E. R. Flynn and D. G. Burke, Phys. Rev. C 17, 501 (1978).

[10]F. T. Baker, A. Scott, T. H. Kruse, W. Hartwig, E. Ventura, and W. Savin, Nucl. Phys. A266, 337 (1976); I. Y. Lee, D. Cline, P. A. Butler, R. M. Diamond, J. O. Newton, R. S. Simon, and F. S. Stephens, Phys. Rev. Lett. 39, 684 (1977); I. Y. Lee, private communication.

[11]S. W. Yates, A. Khan, and M. Mirzaa, Bull. Am. Phys. Soc. 24, 836 (1978); S. W. Yates, private communication.

[12]P. T. Deason, R. M. Ronningen, C. H. King, J. A. Nolen, T. L. Khoo, and F. M. Bernthal, Bull. Am. Phys. Soc. 24, 685 (1979); P. T. Deason, R. M. Ronningen, private communication.

[13]A. H. Wapstra and K. Bos, At. Data Nucl. Data Tables 19, 175 (1977).

[14]P. T. Deason, C. H. King, T. L. Khoo, J. A. Nolen, and F. M. Bernthal, Phys. Rev. C 20, 927 (1979).

[15]C. M. Lederer and V. S. Shirley, *Table of Isotopes*, 7th ed. (Wiley, New York, 1978), p. 1270.

[16]P. D. Kunz (unpublished).

[17]E. R. Flynn, D. D. Armstrong, J. G. Beery, and A. G. Blair, Phys. Rev. 182, 1113 (1969).

[18]F. G. Perey, Phys. Rev. 131, 745 (1963).

[19]E. R. Flynn and O. Hansen, Phys. Lett. 31B, 135 (1970).

[20]M. Finger, R. Foucher, J. P. Husson, J. Jastrzebski, A. Johnson, G. Astner, B. R. Erdal, A. Kjelberg, P. Patzelt, A. Hoglund, S. G. Malmskog, and R. Henck, Nucl. Phys. A188, 369 (1972).

[21]W. E. Cleveland and E. F. Zganjar, Z. Phys. A 279, 195 (1976).

[22]K. Kumar and M. Baranger, Nucl. Phys. A122, 273 (1968).

[23]R. F. Casten and J. A. Cizewski, Nucl. Phys. A309, 477 (1978).

[24]J. Meyer-ter-Vehn, Phys. Lett. 84B, 10 (1979).

[25]U. Götz, H. C. Pauli, K. Alder, and K. Junker, Nucl. Phys. A192, 1 (1972).

[26]K. J. Weeks and T. Tamura, Phys. Rev. Lett. 44, 533 (1980); K. J. Weeks and T. Tamura, Phys. Rev. C 22, 1323 (1980); K. J. Weeks, private communication.

[27]C. Ellegaard, J. D. Garrett, and J. R. Lien, Nucl. Phys. A307, 125 (1978).

[28]D. Breitig, R. F. Casten, W. R. Kane, G. W. Cole, and J. A. Cizewski, Phys. Rev. C 11, 546 (1975).
[29]A. Arima and F. Iachello, Phys. Rev. C 16, 2085 (1977).
[30]H. L. Sharma and N. M. Hintz, Phys. Rev. C 13, 2288 (1976).
[31]O. Scholten (unpublished).
[32]A. Arima, T. Otsuka, F. Iachello, and I. Talmi, Phys. Lett. 66B, 205 (1977).
[33]R. Bijker, A. E. L. Dieperink, O. Scholten, and R. Spanhoff, Nucl. Phys. A344, 207 (1980); A. E. L. Dieperink, private communication.
[34]J. N. Ginocchio, Phys. Lett. 85B, 9 (1979); Ann. Phys. (N.Y.) 126, 234 (1980).
[35]T. Holstein and H. Primakoff, Phys. Rev. 58, 1098 (1940).
[36]B. F. Bayman and A. Kallio, Phys. Rev. 156, 1121 (1967).
[37]A. Bohr and B. R. Mottelson, *Nuclear Structure* (Benjamin, New York, 1975), Vol. II, p. 641.
[38]R. E. Anderson, P. A. Batay-Csorba, R. A. Emigh, E. R. Flynn, D. A. Lind, P. A. Smith, C. D. Zafiratos, and R. M. DeVries, Phys. Rev. C 19, 2138 (1979).